ARTICLE IN PRESS
Journal of the Saudi Society of Agricultural Sciences (2015) xxx, xxx–xxx

King Saud University
Journal of the Saudi Society of Agricultural Sciences
www.ksu.edu.sa
www.sciencedirect.com

FULL LENGTH ARTICLE

Geo-spatial approach for soil salinity mapping in Sego Irrigation Farm, South Ethiopia

Shegena Zewdu [a], K.V. Suryabhagavan [a,*], M. Balakrishnan [b]

[a] School of Earth Sciences, Addis Ababa University, P.O. Box No. 1176, Addis Ababa, Ethiopia
[b] Department of Zoological Sciences, Addis Ababa University, P.O. Box No. 1176, Addis Ababa, Ethiopia

Received 14 April 2014; revised 1 December 2014; accepted 15 December 2014

KEYWORDS
Empirical model;
Geospatial tools;
Irrigation;
NDSI;
Overlay salinity model;
Salinization

Abstract Soil salinization is a major problem affecting productivity of irrigated lands in arid and semi-arid areas. Managing salinity to minimize environmental impact is a prerequisite for sustainable irrigated agriculture. The objective of this study was to assess the level of salinity in Sego irrigated farm, Ethiopia and to map temporal and spatial distribution of salt affected soils to support management programmes. The study employed normal image classification, and developing models from ECe *vs* NDSI and thematic layers to map soil salinity, using geospatial tools. Multi-temporal Landsat TM images of 1984, 1995 and 2010 were used to detect salinity affected areas in the study area. Results of the study revealed that around 6 ha of the area gets moderately to strongly salinized per year. Empirical model developed from ECe *vs* NDSI of 2010 image using regression analysis revealed the coefficient of relation as 66%. The model was extended for the whole area, and revealed that 2.0% of the study area was strongly saline and 54.7% of the area was non-saline. Overlay model developed from water table, land form, land management type and land-cover has revealed that 11.2% of the study area was non-saline, whereas 47.2% and 3.0% was moderately and strongly saline, respectively. Validation of the models was made to test their predication capability and the overlay model has revealed better correlation coefficient of 67.3% to the measured ECe. Most of the salt affected areas were on shallow water table. Cambisols and fluvisols were greatly affected by salinity. The results indicate that long-term irrigation activities would affect agricultural potentiality of the area in the future, and geospatial tools are efficient and feasible for detecting salt affected areas from satellite images and thematic maps.

1. Introduction

Soil salinization in irrigated lands is becoming an increasing problem affecting global agricultural production and sustainable utilization of land resources, especially in arid and semi-arid regions. Soil degradation due to salinity and sodicity is increasing at an alarming rate of endangering the agricultural practices (Metternicht, 2003; Astaraei et al., 2008; Zheng et al.,

* Corresponding author. Tel.: +251 911998588.
E-mail address: drsuryabhagavan@gmail.com (K.V. Suryabhagavan).
Peer review under responsibility of King Saud University.

Production and hosting by Elsevier

http://dx.doi.org/10.1016/j.jssas.2014.12.003

2009; Rongjiang and Jingsong, 2010). It is a severe environmental hazard that impacts growth of several crop varieties. Statistics on the extent of world salt affected areas vary; however, general estimates are close to one billion hectares, which represent about 7% of the earth's continental extent. More than 120 countries are confronted to a smaller or to a greater degree with the problem of soil salinity (Al-Khaier, 2003). Land degradation, which is the product of a complex interaction of several variables, reduces the potential capability of soils to produce goods and services. Semi-arid regions are under high pressure to produce food for their rapidly increasing populations. The consequent changes in land-use mainly due to agricultural intensification together with harsh climatic conditions including global climate change, have accelerated land degradation process, which has already caused yield reduction in many parts of the arid world. Therefore, the need for detecting salinization and land degradation along with assessing its severity at any given time becomes vital. According to Beshir and Bekele (2007), some of the problems of large scale irrigation systems in Ethiopia are lack of awareness among farm officials, and policy problems. Further, irrigation systems are affected by water logging, deterioration of canal capacity and salinity. The main sources of salinity are shallow ground water tables, natural saline seeps irrigation waters, source from marine origin and intensive use of chemicals in agricultural practices. In arid and semi-arid regions, evaporation exceeds precipitation, which causes upward movement of dissolved alkaline salts from the ground water. At the same time, rain water causes downward movement of salts. The net result is deposition of the translocated cations at or very near the soil surface, which is the root zone of most plants. Countries like Ethiopia, where arid and semiarid climatic zones occupy over 60% of the land area, development of technology to control and mitigate salinity and sodicity is an important issue for modern agricultural development and management (Beshir and Bekele, 2007). Land-use pattern changes in relation to the increase of human population density and expansion of irrigated cultivation leading to salinization of the soils lowering productivity have already been reported (Zewdu et al., 2014).

Ethiopian Irrigation Development Program has proposed 26 medium and large scale irrigation projects to be implemented. Due to topographic reasons, most of the already established or proposed large scale irrigation schemes are in the lowlands of the nation, where major river basins such as Awash, Blue Nile, Wabe Shebelle river basins and the Great Rift Valley basin are located. Over 11 million ha of land in the arid, semi-arid and desert regions of Ethiopia is known to be already salt affected (Wlachew et al., 2008). Large areas of the Awash river basin, especially the middle and lower parts of the basin are saline or sodic or in saline sodic phase, and thus potentially exposed to salinization and sodicity. Detection of soil degradation by means of conventional soil survey requires a great deal of time, but remote sensing techniques offer the possibility for mapping and monitoring such processes more quickly and economically. However, to assess the accuracy of the ability of satellite images to map and monitor salinity, it is necessary to compare them with field measurements of salinity (El-haddad and Garcia, 2006). Geospatial and remote sensing approaches are efficient in accuracy, cost effectiveness, speed, and labour savings for delineating salt affected soils (Al-Mulla, 2010; Mohamed et al., 2012). Therefore, the objective of the present study was to assess the level of salinity in Sego irrigated farm and to map the distribution of the problem in the area through application of salt indices and developing different salinity mapping to identify the best mapping method, useful for effective management and strategies to predict and overcome the problem.

2. The study area and methods

2.1. The study area

The study area is located in the Southern Nations Nationalities and Peoples Regional State of Ethiopia (SNNPRS) at about 24 km south of Arba Minch town, extended on both sides of Arba Minch–Konso asphalt road. Geographically, it is bounded by latitudes 5°48′12″–5°54′9″N and longitudes 37°25′9″–37°30′50″E with an area coverage of 6747 ha (Fig. 1). This is a flood plain bounded area by Lake Chamo in the eastern and southern directions, while its northern and western directions are bounded by mountains. The area is drained by Sile and Sego rivers, which empty into Lake Chamo.

There is an abrupt change in the topography about 5 km downstream of the dam site, where Sego and Sile rivers emerge onto a plain bordering Lake Chamo (at the command area). This is the lowest part of the Ethiopian Rift Valley in the area at an elevation of about 1100–1250 m asl. Meteorological data were obtained from the Ethiopian National Meteorological Agency (NMA). The study area is characterized by hot sub-humid lowlands in the eastern and northern parts and warm sub-humid lowlands to warm humid lowlands in the western and north-western parts of the watershed. The annual evapotranspiration is almost uniformly distributed throughout the year. Seasonal temperature variation is only marginal. At Arba Minch, the mean monthly temperature is 23.9 °C, varying between 22.7 °C in July and 25.7 °C in March. Rainfall distribution in the study area is bimodal. A long rainy season occurs from the beginning of March to the end of May with a maximum rainfall recorded in April (219 mm), and a short rainy season from mid-August to mid-October, during which the maximum rainfall recorded was in October (120 mm).

The study area is characterized by eight major soil types. These are cambisols, fluvisols, luvisols, vertisols, gleysols, solonetz, solonchaks and leptosols. Cambisols dominates the soil type of the area, which covers about 54% of the command area, followed by fluvisols. The parent material is alluvial river deposits and colluvial materials developed over the old lacustrine deposits (FAO, 2009).

2.2. Methods

To assess spatial distribution of saline soils with respect to soil type, map of salt affected soils was overlaid with soil type map. For this purpose, map showing eight major FAO soil classes of scale 1:10,000 was obtained from Generation Integrated Rural Development Consultant (GIRDC), based on the soil survey 2009. The present study was conducted using Landsat TM satellite data of 1984, 1995 and 2010 (path 169 and row 056) obtained from global land cover. The satellite data were digitally rectified and processed using the ERDAS Imagine 9.2. Digital elevation models (DEM) of 30 meter resolution

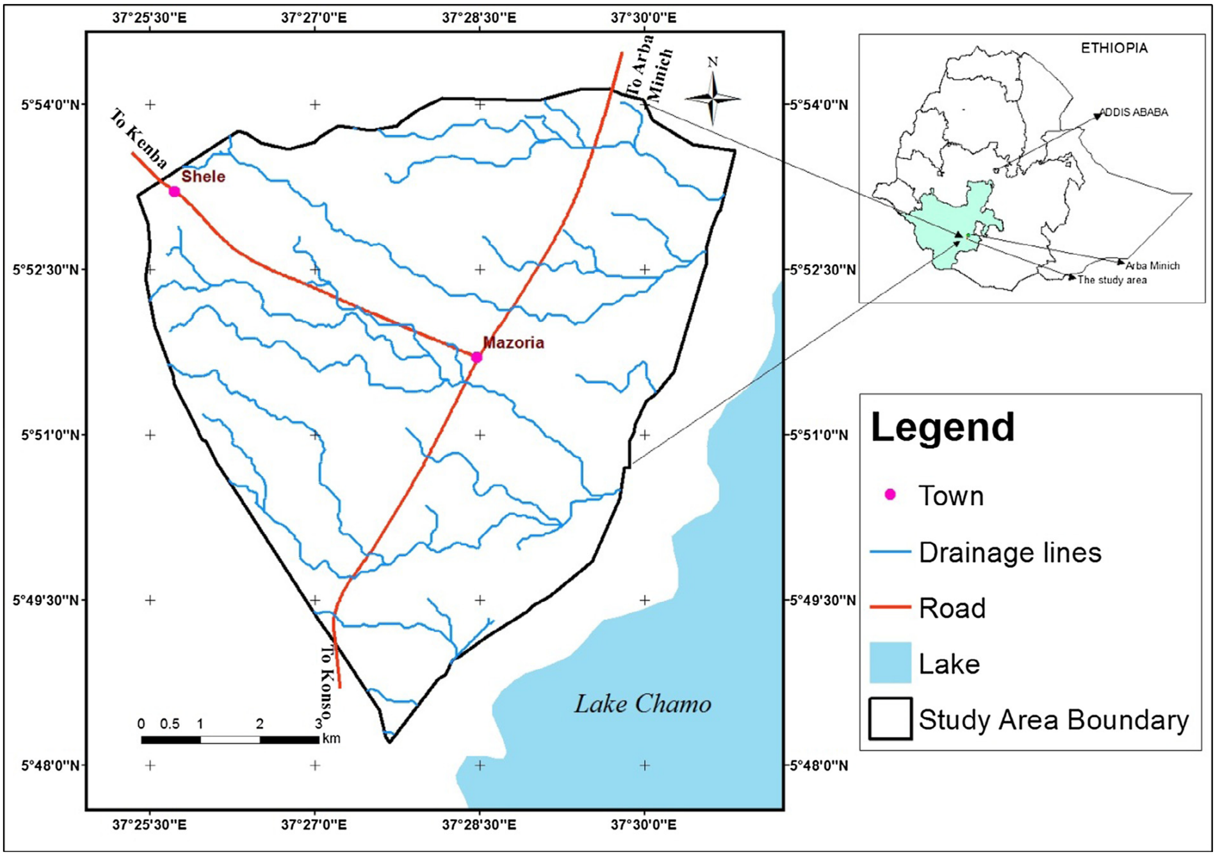

Figure 1 Location map of the study area.

were also used. These data sets were analyzed and salt affected areas were mapped using geo-spatial approach. ERDAS Imagine 9.2 and the ArcGIS 10.1 were used as main GIS packages for building models and running functions such as input, output, analysis and processing. Ethiopian mapping agency (EMA) toposheet (0537 A2) of 1:50,000 scale pertaining to the study area was used for geo-referencing of satellite images, creation of the study area map, and validation of the ground truth. The salt affected area boundaries extracted from the working plan of the Government Department were transferred onto toposheet, and different administrative boundaries and transport network were generated. Soil salinity of the study area was mapped by overlay soil salinization model and salinity model from measured electrical conductivity (ECe) and spectral reflectance, and finally validation and comparison of the methods were made.

2.2.1. Salinity model from measured ECe and spectral reflectance

To assess the spatial distribution of ECe and to predict salinity level at different locations, regression analysis was made, based on ECe point data and Normalized Difference Salinity Index (NDSI) generated from Landsat image 2010. For this analysis, a total of 84 samples (ECe points) were used based on the result of soil field survey by HALCROW-GIRDC, 2009. Salinity for the study area, expressed in ECe value, was found as point data to represent the value at the sampling location. Attempt was made to predict ECe values at unsampled locations through regression analysis. This was done by distributing the ECe sample points on NDSI generated from images of 2010 in the ArcMap. The corresponding value of NDSI for ECe point value was extracted using spatial analyst tool (extract values to points) in the ArcGIS environment, the corresponding ECe values were plotted on scatter diagram and the best fit line and equation were determined (Eq. 1 below). Based on the equation, regression analysis model was developed using model builder in the ArcGIS environment to predict soil salinity level for the whole area in the form of raster map.

$$\text{Salinity} = 58.06x^2 + 32.63x + 6.63 \tag{1}$$

where x is spectral reflectance/NDSI.

2.3. Soil salinization model

Ground water level, landform, land management type, soil texture and land cover were used for soil salinization model. All factor layers were resampled to 30 m cell size to the resolution of DEM and Landsat image and reclassified. Scale values ranging from 1 to 3 were assigned to each of the classes of the factor layers based on their susceptibility to salinization process, where scale value 1 shows the lowest susceptibility and value 3 the highest.

Multi-Criteria Evaluation was used in weighted overlay analysis, where weights of all the layers were combined to sum one. Weightings that represent the relative importance

Please cite this article in press as: Zewdu, S. et al., Geo-spatial approach for soil salinity mapping in Sego Irrigation Farm, South Ethiopia. Journal of the Saudi Society of Agricultural Sciences (2015), http://dx.doi.org/10.1016/j.jssas.2014.12.003

Table 1 Pair-wise comparison of factor layers Principal Eigen vector of the pair-wise comparison matrix.

Layer/factor	Water table level	Landform	Land management	Land cover	Soil texture	Weight
Water table level	1	–	–	–	–	0.36
Landform	1/2	1	–	–	–	0.25
Land management	1/2	1/2	1	–	–	0.18
Land cover	1/3	1/2	1/2	1		0.12
Soil texture	1/3	1/3	1/2	1/2	1	0.09

of concerns were developed. The procedure employed to establish weight value for each of the layers involved in the overlay analysis was pair-wise comparisons in the IDRISI Andes software version 15.0. The comparison was based on relative importance of the two criteria involved in determining salinity vulnerability of the area. Hence, every possible pairing was compared and the ratings were recorded into a pair-wise comparison matrix. The resulting weight from pair-wise comparison for each of the soil salinity factors is shown in Table 1. To generate the map of salt affected soils from the weighted overlay analysis of soil salinization model, the cell value of each model parameter was multiplied by its respective weight (Eq. 2), and the resulting cell values were added to produce the final output raster, showing the level of soil salinity. To generate the final map of salt affected soils, the raster map was reclassified into four classes, ranging from 1 to 4. In the output raster, the higher value indicates areas of strong salinity level, whereas low raster value indicates less salinity level.

$$\begin{aligned}\text{Salinity} = {} & (0.36 \times \text{Ground water level}) + (0.25 \times \text{Landform}) \\ & + (0.18 \times \text{Land management}) + (0.12 \times \text{Land cover}) \\ & + (0.09 \times \text{Soil texture}) \end{aligned} \tag{2}$$

Validation and comparison of empirical model derived from Soil ECe *vs* NDSI and overlay salinity model of the four factor layers were made. This was done by plotting the ECe value and raster value of salinity map from empirical model and overlay model on scattered diagram. Then correlation between ECe value and raster value of each of the models was derived. A flow chart of the methodology is presented in Fig. 2.

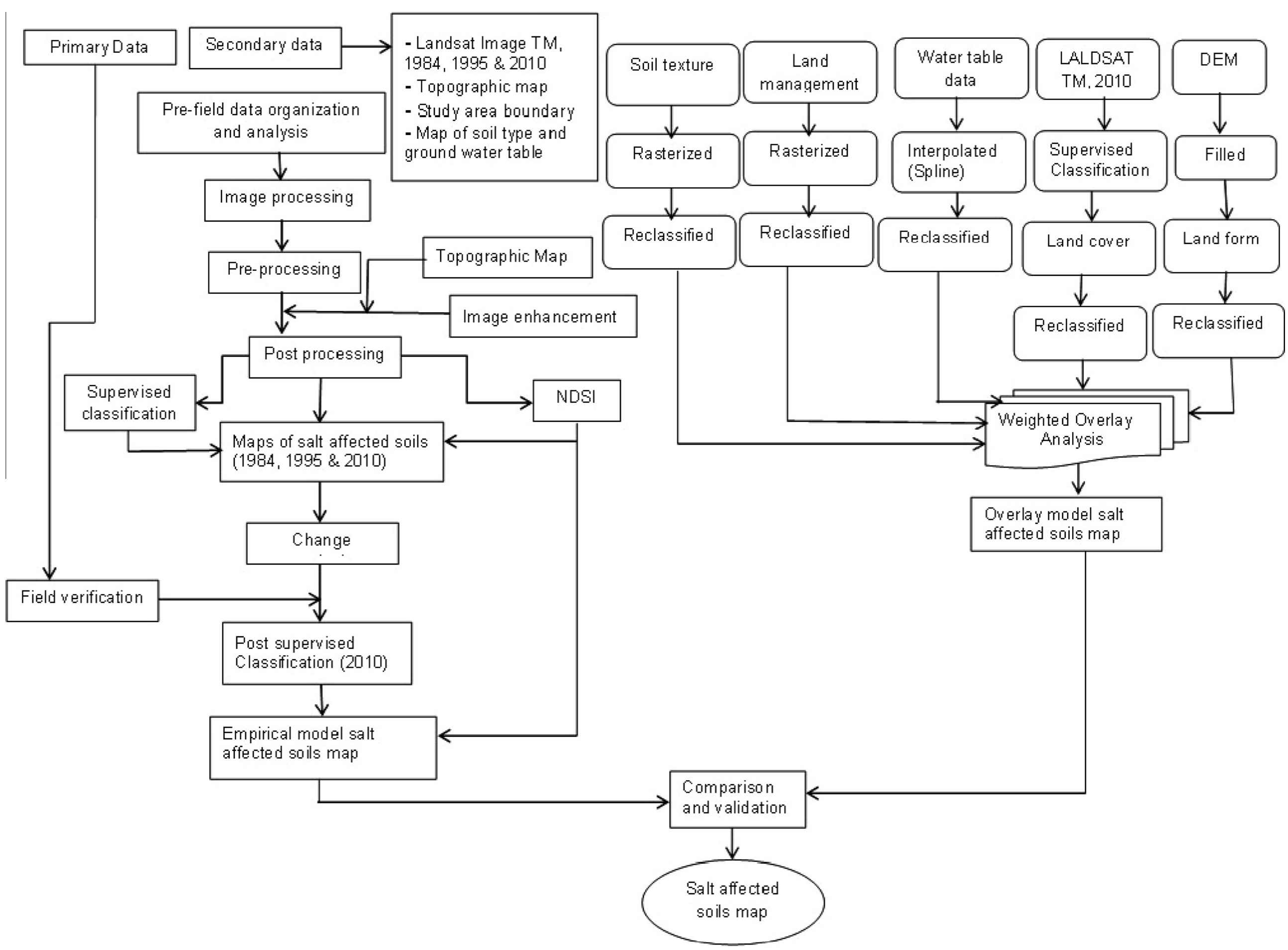

Figure 2 Flow chart showing geo-spatial approach of the developed salinity model.

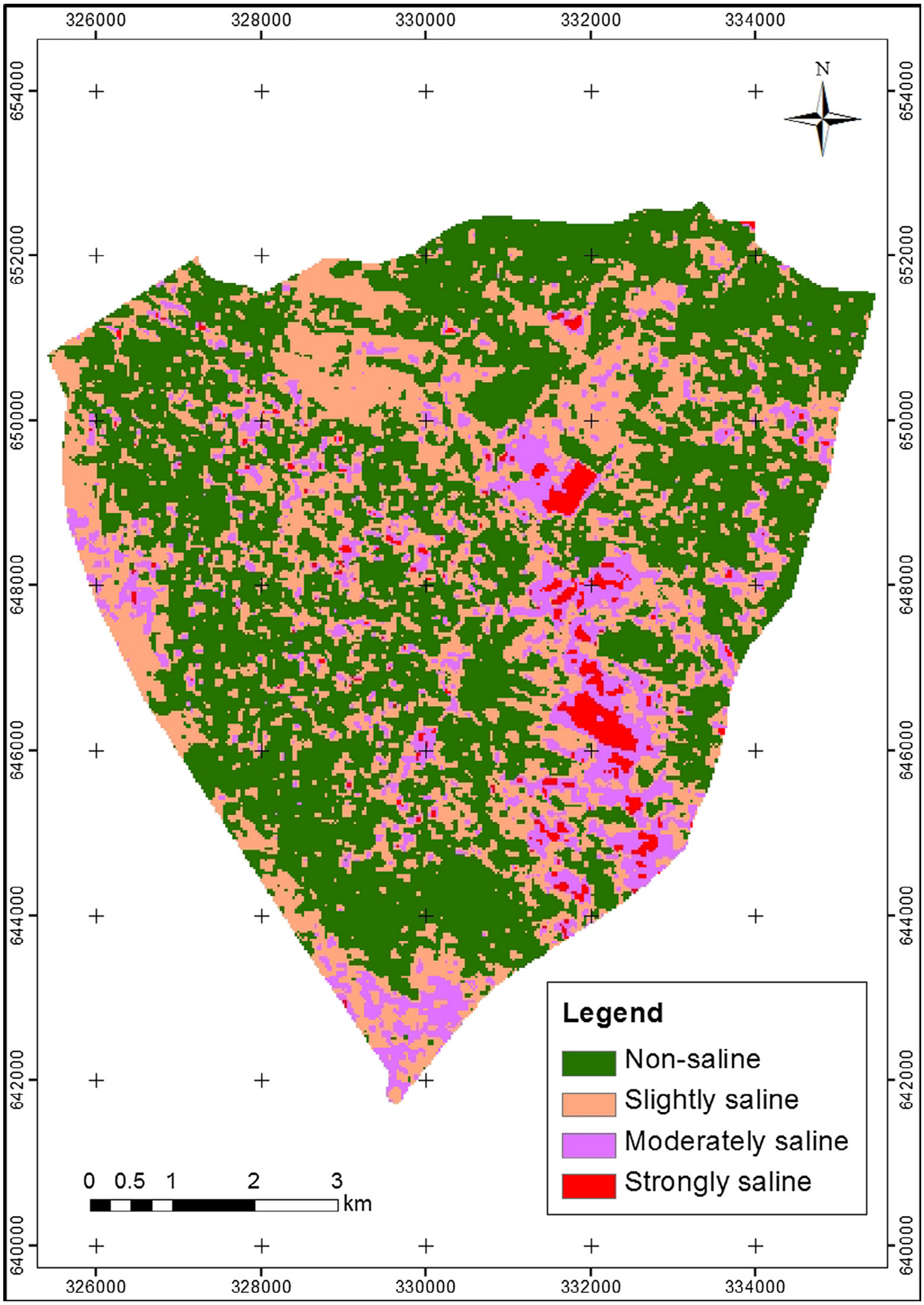

Figure 3 Salt affected soil map derived from NDSI.

3. Results

3.1. Soil salinity (ECe) and NDSI

The map of salt affected soils derived from empirical model revealed four classes of salinity levels with different extents of area (Fig. 3), viz. non-saline, slightly saline, moderately saline and strongly saline soils. Non-saline soil area was the largest in extent (3692.7 ha), which was 54.7% of the total area (Table 2). Strongly saline soil covered 2.0%, which was mainly in the central part of the study area. Spatially, it coincided with those derived from supervised classification and NDSI classification except the variation in the area coverage. The model revealed some new patchy areas of strong salinity in the northern and western edges of the study area. Slightly saline and moderately saline soils covered 32.6% and 10.6%, respectively, and found scattered throughout the study area.

The empirical model of ECe *vs* NDSI offered 66% coefficient determination. Most of the measured ECe points

Table 2 Area extent of soil salinity level derived from NDSI.

Salinity level (mS/cm)	Salinity extent	Area (ha)	Area (%)
2.05–4	Non-saline	3692.7	54.7
4–8	Slightly saline	2202.0	32.6
8–15	Moderately saline	715.0	10.6
> 15	Strongly saline	136.9	2.0
Total	6746.5	100	

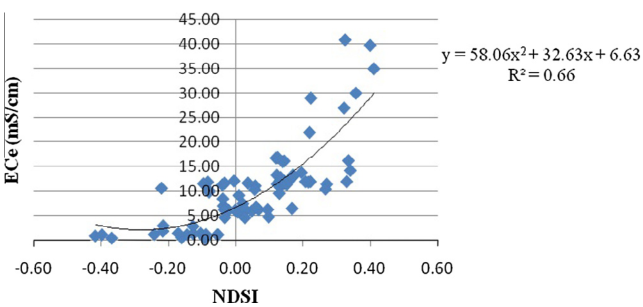

Figure 4 Regression analyses model between ECe and NDSI.

concentrated in the lower part of the NDSI value (Fig. 4), but some of the NDSI values indicated high level of salinity in the area.

3.2. Overlay salinization model

Water table had higher degree of influence (about 47%), followed by landform (28%). Land management and land-cover have 14% and 11% influence, respectively. The result of overlay soil salinization model revealed four levels of soil salinity such as strongly saline, moderately saline, slightly saline and non-saline with different extents (Table 3 and Fig. 5). Strongly saline area contributed for 2.8%, which concentrated in the central part of the study area, slightly and non-saline areas account for 31.2% and 26.6%, respectively, where land management was largely under the State farm, characterized by sparse vegetation, shallow water table and low laying landform. Moderately saline areas were concentrated in the central and eastern parts of the study area, where water table level was moderate to shallow, characterized by low laying lands along the shore of Lake Chamo.

3.3. Validation and comparison of the models

The test for validity of empirical model showed high correlation (66.0%) between measured ECe value and salinity derived from the model (Fig. 6). The correlation between measured ECe value and salinity derived from the model was also found correlated (67.3%). Coefficients of correlation showed that both models were of approximately equal validity. However, the overlay model was better compared to the empirical model. Hence, prediction of salt affected areas can be executed using the overlay soil salinization model developed from the five factor layers (water table level, landform, land management type, soil texture and land cover).

Direct validation from the field with supporting photos showed the salinity status in the study area. Crystalline salts were clearly seen on the land surface in some of the areas (Fig. 7). As a result, currently, most of these areas are abandoned from cultivation, whereas nearby areas are left as bare land and some areas are used for grazing.

3.4. Soil type

Cambisoil dominated the study area to an extent of 3683.3 ha, which was largely affected by salinity as moderately (25%) and strongly saline (2.3%), respectively (Table 4). The next salt affected soil was fluvisols occurring in the low laying landform under moderate salinity level accounting for 12.8% of the area. Solonchaks and solonetz, which were associated with salt affected soil, were under moderate salinity levels covering 2.4% and 1.9% of the study area, respectively. The rest of the soils were slightly and strongly saline, which collectively accounted for 0.8% of the present study area.

All the non-saline soils (11.2%) were on deep water table depth, whereas 14.6% of these areas were slightly saline (Table 5). Soils on deep water table are not affected by salinity. Out of the 3781.7 ha area, with shallow water table depth, 16.7% and 36.4% were slightly and moderately saline, respectively. Almost all the strongly saline soils covering an area of about 3% were situated on shallow water table depth.

4. Discussion

In the present study, both the maps of soil salinity showed that moderately and strongly saline soils are largely concentrated in the eastern and central parts, especially the strongly saline soils are in the central part of the study area. The area has been

Table 3 Area extent of salinity classes derived from overlay model.

Salinity class	Area (ha)	Area (%)
Strongly saline	189.2	2.8
Moderately saline	2662.9	39.5
Slightly saline	2103.1	31.2
Non-saline	1791.2	26.6
Total	6746.5	100

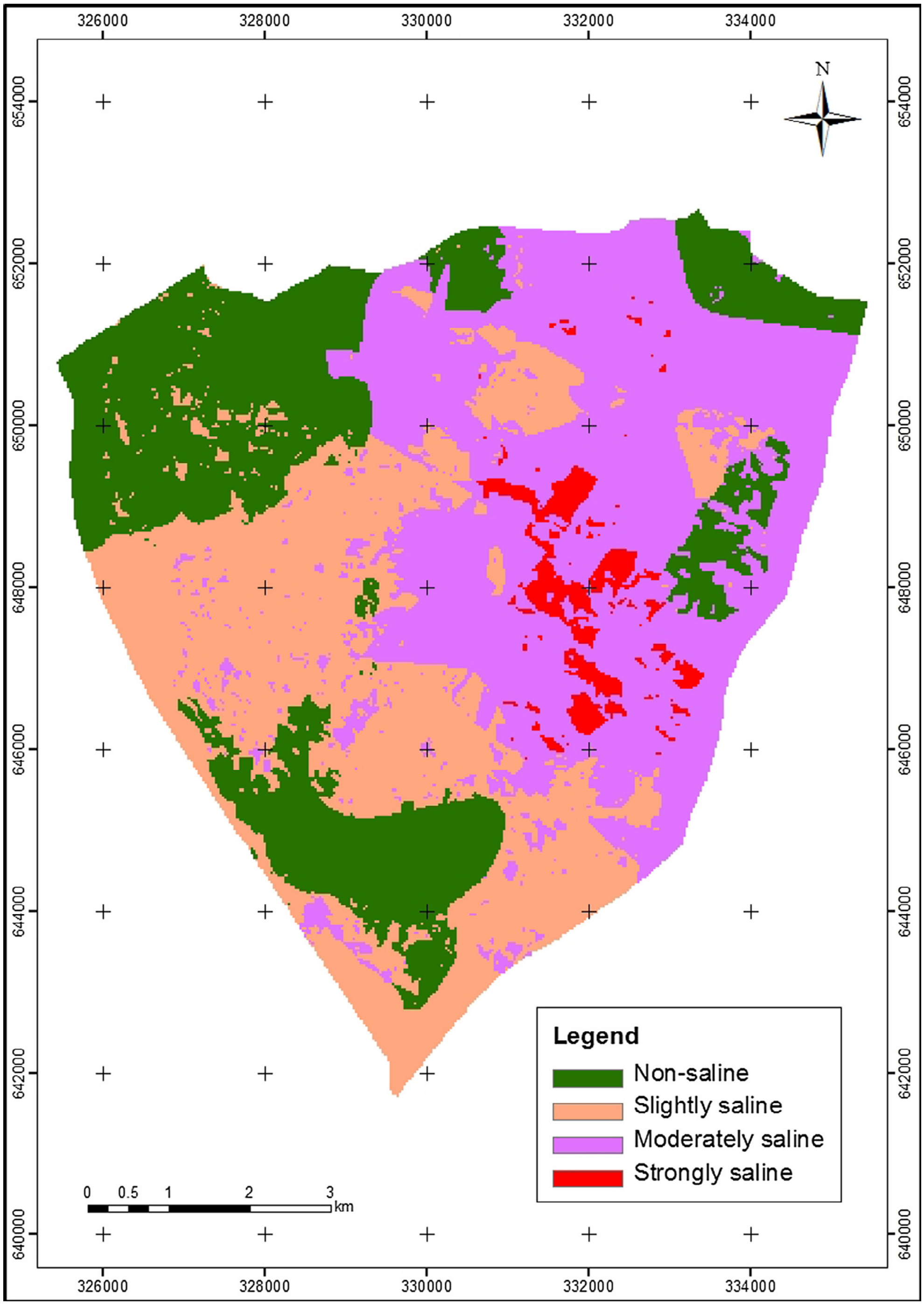

Figure 5 Salt affected soil map derived from overlay model.

under irrigated agricultural practice more than the last two decades, which would be the cause for the soil salinization in the study area.

For a better management of salt affected soils, soil salinity needs to be monitored and mapped, and prediction of salt affected areas can be made using the overlay soil salinization model developed from the five factor layers, *viz*., water table level, landform, land management type, soil texture and the interactions with the vegetation cover in the area (Zheng et al., 2009). This model directly gives the salinity level at any point in the image. Hence, determining the spatial soil salinity potential of Sego Irrigation Farm by integrating GIS functionalities using overlay model is crucial. It is a rapid and reliable method of obtaining information on the spatial distribution of salinity (Madyaka, 2008). The geologic formation of the command area is characterized by a single unit. However, soil texture was used as one layer as the grain size matters the process due to variability in texture and porosity, which affects ground water flow. Water table is one of the most important factors, where salts present in the soil are moved with soil

ARTICLE IN PRESS

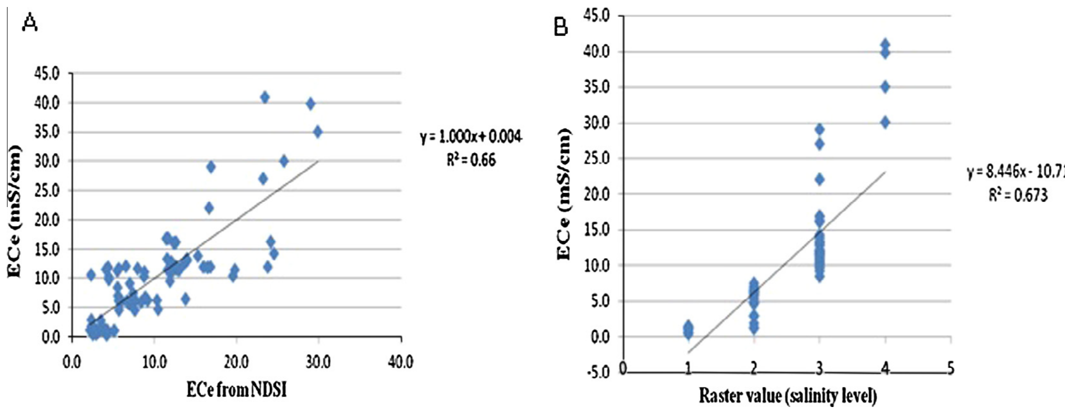

Figure 6 Correlation between measured ECe *vs* NDSI (A) and ECe *vs* raster value of overlay model (B).

Figure 7 Surface salt crystals spread in the central part of the study area.

moisture through capillary actions and become a source of saline soil formation when water table is close to the soil surface and evaporation rate is high (Chaudhry et al., 1996). This indicates that shallow water table and low laying landforms are largely contributing to soil salinity. HALCROW-GIRDC (2009) revealed that groundwater quality indicates stronger salinity levels in the lower parts of the study area, which may be due to salinization from poor water management practices or due to the influence of Lake Chamo on groundwater salinity near the lake shore. Consequently, shallow ground water depth has higher influence on soil salinity rise and higher depth of ground water level has lower influence on soil salinization.

Changes in the salinity levels with reference to the years of irrigation are revealed in the present study area. It is already revealed that in combination with the traditional surveys, the presence of salt in the surface layer of the topsoil can be detected with reasonable accuracy using remote sensing (Abdellatif and Mourad, 2012). Integration of remote sensing with traditional soil surveys and modern soil geo-spatial approaches leads toward a more accurate approach of digital soil salinity mapping (Lagacherie, 2008). Soil salinity maps made from both empirical and overlay techniques have revealed occurrence of salinity in the study area, including variations in the extent of area coverage of the salinity classes as reported earlier (Mccutcheon et al., 2006), and changes in the soil physicochemical properties (Rongjiang and Jingsong, 2010).

In conclusion, geospatial tools are efficient and time saving for mapping and prediction of soil salinity by applying different models. Empirical and overlay salinization models used in this study show that significant extent of area is affected with salt. However, there are variations in the non-saline and mod-

Table 4 Soil salinity distribution with respect to soil type.

Soil type	Soil salinity classes and extents (ha)								Total
	Non-saline		Slightly saline		Moderately saline		Strongly saline		
	Area	Area (%)	Area	Area (%)	Area	Area (%)	Area	Area (%)	Area
Cambisols	611.6	9.1	1223.0	18.1	1693.1	25.1	155.6	2.3	3683.3
Fluvisols	3.8	0.1	741.8	11.0	865.0	12.8	37.7	0.6	1648.2
Gleysols	0.0	0.0	9.5	0.1	37.2	0.6	0.9	0.0	47.5
Luvisols	86.4	1.3	355.3	5.3	231.4	3.4	0.3	0.0	673.3
Solonchaks	0.0	0.0	5.7	0.1	160.1	2.4	0.5	0.0	166.4
Solonetz	0.0	0.0	48.3	0.7	127.0	1.9	4.7	0.1	180.0
Vertisols	0.0	0.0	22.1	0.3	37.9	0.6	0.0	0.0	60.1
Leptosols	52.7	0.8	199.1	3.0	34.8	0.5	0.7	0.0	287.3
Total	754.6	11.2	2604.9	38.6	3186.6	47.2	200.5	3.0	6746.5

Please cite this article in press as: Zewdu, S. et al., Geo-spatial approach for soil salinity mapping in Sego Irrigation Farm, South Ethiopia. Journal of the Saudi Society of Agricultural Sciences (2015), http://dx.doi.org/10.1016/j.jssas.2014.12.003

Table 5 Soil salinity distribution with respect to water table depth.

Water table depth	Soil salinity classes and extents (ha)								Total
	Non-saline		Slightly saline		Moderately saline		Strongly saline		
	Area	Area (%)	Area	Area (%)	Area	Area (%)	Area	Area (%)	
Deep	753.4	11.2	987.9	14.6	35.4	0.5	0.0	0.0	1776.7
Moderate	1.1	0.0	489.6	7.3	696.8	10.3	0.5	0.0	1188.1
Shallow	0.0	0.0	1127.4	16.7	2454.4	36.4	199.9	3.0	3781.7
Total	754.5	11.2	2604.9	38.6	3186.6	47.2	200.5	3.0	6746.5

erately saline areas mapped using the two models. But, the overlay model has better prediction capability than the empirical model. Though the correlation coefficient between measured salinity and the salt affected map derived from the empirical model is less than that of the overlay model, it is a good and efficient method for detecting salt affected areas from satellite images, and hence can be used in similar areas that experience salinization problems.

Conflict of interest

No conflict of interest.

Acknowledgements

The School of Earth Sciences, Addis Ababa University is thanked for funding this study. Generation Integrated Rural Development Consultant deserves special thanks for the support provided during the study. The Sego irrigation farm workers are thanked for providing helpful information. We are also thankful to the anonymous reviewers for their comments, which helped us to improve this manuscript.

References

Abdellatif, D., Mourad, L., 2012. Remote sensing techniques for salt affected soil mapping: application to the Oran region of Algeria. Procedia Eng. 33, 188–198.

Al-Khaier, F., 2003. Soil Salinity Detection Using Satellite Remote Sensing. M.Sc. Thesis. The International Institute for Geo-information Science and Earth Observation. Enschede, Netherlands.

Al-Mulla, Y., 2010. Salinity Mapping in Oman using Remote Sensing Tools: Status and Trends. Monograph on Management of Salt-Affected Soils and Water for Sustainable Agriculture, Oman. pp. 17–24.

Astaraei, Ali Reza., Sanaeinejad, S.H., Mir Hosseini, M.P., Ghaemi, M., Keshavarzi, A., 2008. Evaluation of Vegetation cover and soil indices for saline land classification in Neyshabour Region using ETM+ Landsat. International Symposium on Geoinformatics for Spatial Infrastructure Development in Earth and Allied Sciences. 73−78.

Beshir, A., Bekele, S., 2007. Analysis of irrigation systems using comparative performance indicators: a case study of two large scale irrigation systems in the Upper Awash basin. Oromia Water Works Design and Supervision Enterprise, IWMI-NBEA. In: Proceedings of the Symposium and Exhibition 77−92, Addis Ababa.

Chaudhry, M.R., Ghafoor, A., Qadir, M., Murtaza, G., 1996. Temporal variation in quality of agricultural drainage and Samundri Branch drain effluents. Pakistan J. Soil Sci. 2, 1–2.

El-haddad, A., Garcia, L.A., 2006. Detecting soil salinity levels in agricultural lands using satellite imagery. <http://proceedings.esri.com/library/userconf/proc05/papers/pap1950.pdf.

FAO, 2009. (Food and Agriculture Organization). Global Information and Early Warning System on Food and Agriculture Special Report. Unpublished working report, FAO, Addis Ababa.

HALCROW-GIRDC, 2009. Rift Valley Lakes Basin Integrated Resources Development Master Plan Study Project. Ministry of Water Resources, Federal Government of Ethiopia, Addis Ababa.

Lagacherie, P., 2008. Digital soil mapping: a state of the art. In: Hartemink, A.E., McBratney, A.B., Mendonça-Santos, M.L. (Eds.), Digital Soil Mapping with Limited Data. Elsevier Science, Amsterdam, The Netherlands.

Madyaka, M., 2008. Spatial Modelling and Prediction of Soil Salinization Using SaltMod in the GIS Environment. M.Sc Thesis, International Institute for Geo-information Science and Earth Observation. Enschede, Netherlands.

Mccutcheon, M.C., Farahani, H.J., Stednick, J.D., Buchleiter, G.W., Green, T.R., 2006. Effect of soil water on apparent soil electrical conductivity and texture relationships in a dryland field. Biosyst. Eng. 94, 19–32.

Metternicht, G.I., 2003. Remote sensing of soil salinity-potentials and constraints. J. Remote Sens. Environ. 85, 1–20.

Mohamed, S.I., Mohammad, A.R., Nahid, S., Biswajit, N., Alak, P., 2012. Using geospatial techniques to assess the salinity impact on agricultural landuse: a study on Shyamnagar Upazila, Satkhira. J. Agric. Environ. Int. Dev. 106, 157–169.

Rongjiang, Y., Jingsong, Y., 2010. Quantitative evaluation of soil salinity and its spatial distribution using electromagnetic induction method. Agric. Water Manag. 97, 1961–1970.

Wlachew, S.B., Loulseged, M., Yilma, A.D., 2008. Impact of irrigation on poverty and environment in Ethiopia. Proceedings of the Symposium and Exhibition, Addis Ababa.

Zewdu, S., Suryabhagavan, K.V., Balakrishnan, M., 2014. Land-use/land-cover dynamics in Sego Irrigation Farm, Southern Ethiopia: a comparison of temporal soil salinization using geospatial tools. J. Saudi Soc. Agric. Sci. http://dx.doi:10.1016/j.jssas.2014.03.003.

Zheng, Z., Zhang, F., Ma, F., Chai, X., Zhu, Z., Shi, J., Zhang, S., 2009. Spatiotemporal changes in soil salinity in a drip-irrigated field. Geoderma 149, 243–248.